Resonant tunneling of surface plasmon-polaritons

Sergei Sidorenko and Olivier J. F. Martin

Nanophotonics and Metrology Laboratory Swiss Federal Institute of Technology Lausanne (EPFL)
EPFL-STI-NAM, ELG Station 11 CH-1015 Lausanne, Switzerland
sergei.sidorenko@epfl.ch
http://nam.epfl.ch/

Abstract: The tunneling of surface plasmon-polaritons (SPPs) across an interruption in the metallic film supporting them is numerically investigated in details. Both non-symmetrical and symmetrical geometries are considered. A very high tunneling efficiency is calculated for the long-range surface plasmon in the symmetrical geometry, with an amplitude transmission as high as 80% over a 5 μm gap for a 40 nm thick gold film illuminated at λ=785nm. The transmission is somewhat lower in the non-symmetrical geometry. The coupling between the different SPP modes (radiative and non-radiative) in that geometry is also investigated in detail. This coupling depends periodically upon the length of the gap. Overall, the results indicate that SPPs are not very sensitive to technological imperfections and can survive large waveguide interruptions.

OCIS codes: (240.6680) Surface plasmons; (240.7040) Tunneling; (290.0290) Scattering; (000.4430) Numerical approximation and analysis; (230.7370) Waveguides

References and Links

1. P. Berini, "Plasmon-polariton waves guided by thin lossy metal films of finite width: Bound modes of symmetric structures," Phys. Rev. B **61**, 10484 (2000).
2. P. Berini, "Plasmon-polariton waves guided by thin lossy metal films of finite width: Bound modes of asymmetric structures," Phys. Rev. B **63**, 125417 (2001).
3. W. L. Barnes, A. Dereux, and T. W. Ebbesen, "Surface plasmon subwavelength optics," Nature **424**, 824 (2003).
4. A. V. Zayats, I.I.Smolyaninov, and A. A. Maradudin, "Nano-optics of surface plasmon polaritons," Phys. Rep. **408**, 131 (2005).
5. S. I. Bozhevolnyi, V. S. Volkov, E. Devaux, and T. W. Ebbesen, "Channel plasmon-polariton guiding by subwavelength metal grooves," Phys. Rev. Lett. **95**, 046802 (2005).
6. J. C. Weeber, M. U. Gonzalez, A. L. Baudrion, and A. Dereux, "Surface plasmon routing along right angle bent metal strips," Appl. Phys. Lett. **87**, 221101 (2005).
7. I. Breukelaar and P. Berini, "Long-range surface plasmon polariton mode cutoff and radiation in slab waveguides," J. Opt. Soc. Am. A **23**, 1971 (2006).
8. T. Nikolajsen, K. Leosson, S. I. Bozhevolnyi, "Surface plasmon polariton based modulators and switches operating at telecom wavelengths," Appl. Phys. Lett. **85**, 5833 (2004).
9. R. Charbonneau, N. Lahoud, G. Mattiussi, P. Berini, "Demonstration of integrated optics elements based on long-ranging surface plasmon polaritons," Opt. Express, **13**, 977 (2005).
10. S. I. Bozhevolnyi , T. Nikolajsen, and K. Leosson, "Integrated power monitor for long-range surface plasmon polaritons," Opt. Commun. **255**, 51 (2005).
11. R. Nikolajsen, K. Leosson, I. Salakhutdinov and S. I. Bozhevolnyi, "Polymer-based surface-plasmon polariton stripe waveguides at telecommunication wavelengths," Appl. Phys. Lett. **82**, 668 (2003).
12. J. Seidel, S. Grafström and L. Eng, "Stimulated emission of Surface Plasmons at the interface between a Silver Film and an Optically Pumped Dye Solution," Phys. Rev. Lett. **94**, 177401 (2005).
13. H. Ditlbacher, F. R. Aussenegg, J. R. Krenn, B. Lamprecht, G. Jakopic, G. Leising, "Organic diodes as monolithically integrated surface plasmon polariton detectors," Appl. Phys. Lett. **89**, 161101 (2006).
14. M. U. Gonzalez, J. C. Weeber, A. L. Baudrion, and A. Dereux, "Design, near-field characterization, and modeling of 45° surface-plasmon Bragg mirrors," Phys. Rev. B **73**, 155416 (2006).
15. G. Gagnon, N. Lahoud, G. A. Mattiussi, and P. Berini, "Thermally activated variable attenuation of long-range surface plasmon-polariton waves," J. Lightwave Technol. **24**, 4391 (2006).
16. J. A. Sanchez-Gil and A. A. Maradudin, "Near-field and far-field scattering of surface plasmon polaritons by one-dimensional surface defects," Phys. Rev. B **60**, 8359 (1999).

#81890 - $15.00 USD Received 6 Apr 2007; revised 7 May 2007; accepted 7 May 2007; published 8 May 2007

17. S. I. Bozhevolnyi, I. I. Smolyaninov and A. V. Zayats, "Near-field microscopy of surface-plasmon polaritons: Localization and internal interface mapping," Phys. Rev. B **51**, 17916 (1995).
18. B. Vohnsen and S. I. Bozhevolnyi, "Coupling of surface-plasmon polaritons to directional far-field radiation by an individual surface protrusion," Appl. Opt. **40,** 6081 (2001).
19. J. Seidel, S. Grafström, and L. M. Eng, "Surface plasmon transmission across narrow grooves in thin silver films," Appl. Phys. Lett. **82**, 1368 (2003).
20. J. Seidel, F. I. Baida, L. Bischoff, B. Guizal, S. Grafström, D. Van Labeke, and L. M. Eng, "Coupling between surface plasmon modes on metal films," Phys. Rev. B **69**, 121405 (2004).
21. E. D. Palik, *Handbook of Optical Constants of Solids* (Academic Press, New York, 1985).
22. E. Kretzschmann and H. Raether, Z. Naturforsch. A **23**, 2135 (1968).
23. COMSOL Multiphysics version 3.3.
24. J.-P. Berenger, "A perfectly matched layer for the absorption of electromagnetic waves," J. Comput. Phys. **114**, 185 (1994).
25. R. Mittra and U. Pekel, "A new look at the perfectly matched layer (PML) concept for the reflectionless absorption of electromagnetic waves," IEEE Microwave Guid. Wave Lett. **5**, 84 (1995).

1. Introduction

Today's tremendous interest for the utilization of surface plasmon-polaritons (SPPs) to transmit and process optical information on metallic structures has given rise to a broad variety of guiding structures [1-7], as well as passive and active components [8-15]. For all these structures, a key issue is how a SPP can tunnel between two guiding elements. This has practical implications for the direct coupling between discrete structures, the sensitivity to interruptions and fabrication defects of SPP propagating on a metallic film, the crosstalks between densely packed waveguides, and the coupling between an external optical fiber and a metallic waveguide.

SPP scattering by a defect on the metallic surface have been addressed both theoretically [16] and experimentally [17, 18]. Recently, Seidel *et al.* have observed that an interruption in a metallic film where a SPP propagates can lead to the excitation of additional SPP modes [19, 20]. Scanning near-field optical (SNOM) images revealed this excitation in the form of a beating between the original mode and that created by the interruption [see Fig. 1 in Ref. 20].

In the present work, we study in detail this effect and on the one side investigate the conditions (metal thickness t and gap length d, Fig. 1) under which the surface plasmon can tunnel across an interruption in a metallic waveguide. On the other side, we explore the crosstalks between the original mode and that created by the interruption. Furthermore, both non-symmetrical and symmetrical geometries are considered.

2. Numerical simulations and results

There exist two main classes of environments for plasmonic structures: symmetrical geometries, where the metallic waveguide is embedded between two dielectric media with the same permittivity and non-symmetrical geometries, where the metallic waveguide is deposited on a substrate and covered with a material with another permittivity, generally air or water. We shall first concentrate on this geometry, where the field of the SPP can be measured experimentally using near-field optical microscopy [17-20].

2.1. Non-symmetrical geometry

The geometry of the system is shown in Fig. 1. A thin gold film with permittivity ε_{Au}=-24.57-1.79*i at the illuminating wavelength λ=785nm [21] is deposited on a dielectric glass substrate with refractive index n_{glass}=1.47. Two SPP modes can propagate in that system, as illustrated in Fig.1. The first mode has its maximum intensity at the metal-air interface, Fig. 1(a); it is a radiative mode, which can be excited by total internal reflection [22]. The other mode is non-radiative and has its maximum intensity at the metal-substrate interface, Fig. 1(b). For a given geometry and excitation wavelength, these two SPP modes are entirely characterized by their propagation constants, which can be expressed in terms of the vacuum wave number $k_0=2\pi/\lambda$. At the considered illumination wavelength λ=785nm for a t=50 nm thick gold film, the propagation constants read k_{air}=1.02-0.0028*i for the air mode and $k_{substrate}$=1.55-0.0069*i for the substrate mode. The imaginary part of the propagation constant

#81890 - $15.00 USD Received 6 Apr 2007; revised 7 May 2007; accepted 7 May 2007; published 8 May 2007

accounts for the damping of the mode as it propagates on the metallic film. Hence the substrate mode decays 2.5 times faster than the air mode.

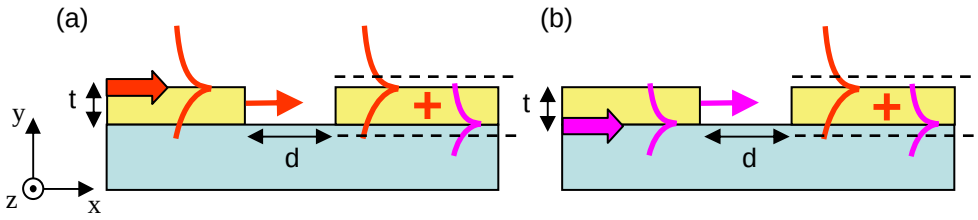

Fig. 1. Sketch of a metallic waveguide with thickness *t* and an interruption *d*. Two SPP modes can propagate in that system. (a) Excitation with an air mode and (b) with a substrate mode. For clarity, modes reflected backwards at the interfaces are not shown.

The finite element method is used to study the influence of an interruption in the metal on the SPP propagation [23]. For SPPs propagating on a metallic film, the entire problem can be reduced to a scalar wave equation for the sole magnetic field component H_z (Fig. 1). Key to the accurate simulation of this system is the careful choice of the boundary conditions at the edges of the computation window. Especially for the problem under study where some of the plasmon energy will be radiated when the SPP scatters over the interruption in the metallic film. Perfectly matched layers are therefore implemented following the approach described in Refs. [24] and [25]. As excitation, the field distribution associated with either the air or the substrate SPP mode is used.

Figure 2 shows the amplitude distribution of the magnetic field when an air mode propagates from the left on a t=50 nm thick gold film with a d=700 nm interruption starting at x=-4 μm. Notice the standing wave pattern in front of the gap, caused by the interaction of the SPP with that reflected at the interruption. Strong scattering both into air and into the substrate is visible in this figure. In the gap, the field propagates freely with wave numbers k_0 in the air and k_{glass}=1.47. After the interruption, the propagation of SPPs on the metallic waveguide is clearly visible, indicative that some of the initial energy has tunneled through the gap.

The movie linked to Fig. 2 shows the tunneling of the SPP when the interruption length varies from d =50 nm to d =4.7 μm (the interruption always starts at x=-4 μm and an air mode is used for excitation). Note in this movie how the transmitted plasmon above the metallic film decreases for large interruptions. Also the scattering in the substrate becomes increasingly important for gaps larger than about d =500 nm. Finally, a beating is visible under the metallic film for gaps up to approximately d =1 μm.

#81890 - $15.00 USD Received 6 Apr 2007; revised 7 May 2007; accepted 7 May 2007; published 8 May 2007

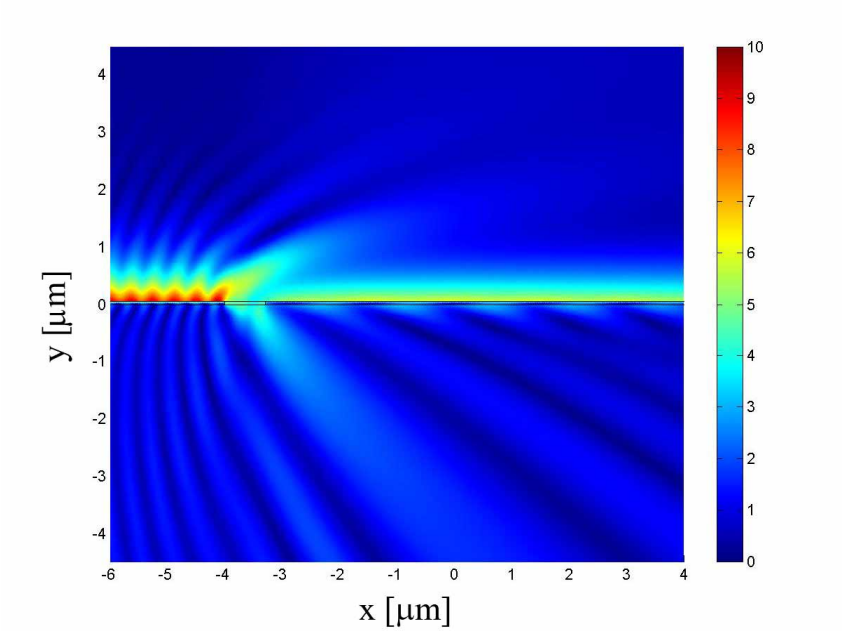

Fig. 2. Amplitude of magnetic field when an air SPP mode is propagating on a t=50 nm thick gold film with a d=700 nm interruption, see Fig. 1(a). The movie shows the field distribution for interruptions between d=50 nm and d=4.7 μm.

To investigate this system in greater detail, we show in Fig. 3 the amplitude of the magnetic field 5 nm below, Fig. 3(a), and 5 nm above, Fig. 3(b), the metallic film (see the dashed lines in Fig. 1). Hence, Fig. 3(a) emphasizes the field associated with the substrate mode, while Fig. 3(b) that of the air mode. Remark that the period of the standing waves in front of the gap in Fig. 3 perfectly matches half the wavelength of the SPP air mode used for illumination. The behavior of the transmitted field is however quite different between Figs. 3(a) and 3(b): the former exhibits a strong rise of the field amplitude after the gap, while the latter shows a decrease of the field. Thus, the field amplitude above the film decreases, while the field amplitude below the film increases. This indicates that some of the energy from the illumination mode (air mode) has been transferred to the substrate mode upon tunneling through the gap. The excitation of this substrate mode is also evidenced in the right part of Fig. 2, where strong scattering into the substrate indicates the presence of a short-lived mode.

Furthermore, a figure of interference is visible on the right of the interruption in Fig. 3. This phenomenon, which is also observed experimentally [19, 20], is caused by the interference between the two SPP modes now propagating on the metallic film. As a matter of fact, the period of this interference p=1480 nm perfectly matches the difference of the corresponding propagation constants $k_{substrate}$ and k_{air}.

#81890 - $15.00 USD Received 6 Apr 2007; revised 7 May 2007; accepted 7 May 2007; published 8 May 2007

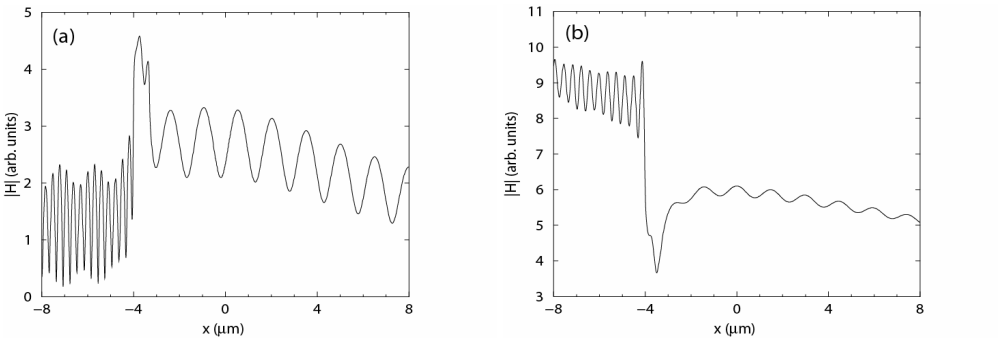

Fig. 3. Amplitude of the magnetic field (a) 5 nm below and (b) 5 nm above the metallic film (see the dashed lines in Fig. 3).

To quantify the tunneling through the gap and investigate the influence of different parameters such as the gap length d and the thickness t of the metallic film, we measure the average amplitude of the transmitted magnetic field at a distance x=6 μm. The average amplitude must be taken since the interference of the air and dielectric modes creates an oscillation of the field amplitude. This average is obtained by exponentially fitting the magnetic field amplitude between x=5 μm and x=7 μm and taking the field value of the fit at x=6μm. This value is further normalized to the amplitude of the field at the same location without any interruption in the film.

Figure 4 shows the transmitted amplitude as a function of the length d of the film interruption, 5 nm above the metallic film, in the air Fig. 4(a), and 5 nm below the metallic film, in the dielectric substrate Fig. 4(b). The system is illuminated with the air mode and different metal thicknesses t are considered. For the field above the metallic film, Fig. 4(a), the transmitted magnetic field amplitude decays exponentially with increasing interruption length. This corresponds to the tunneling of the air SPP mode over the gap. It is quite remarkable that the original mode can tunnel over several microns.

The behavior of the field under the metal in the dielectric is however quite different, as illustrated in Fig. 4(b). Now the magnitude of the average magnetic field varies periodically with the length d of the gap. Note that this figure corresponds to the excitation of the substrate mode by the scattering of the air mode through the gap. The period b_1 of the oscillations visible in Fig. 4(b) appears to be given by the beating between the scattered waves propagating in the glass and in the air over the distance of the gap: $b_1=\lambda_0/(n_{glass}-1)=1654$ nm.

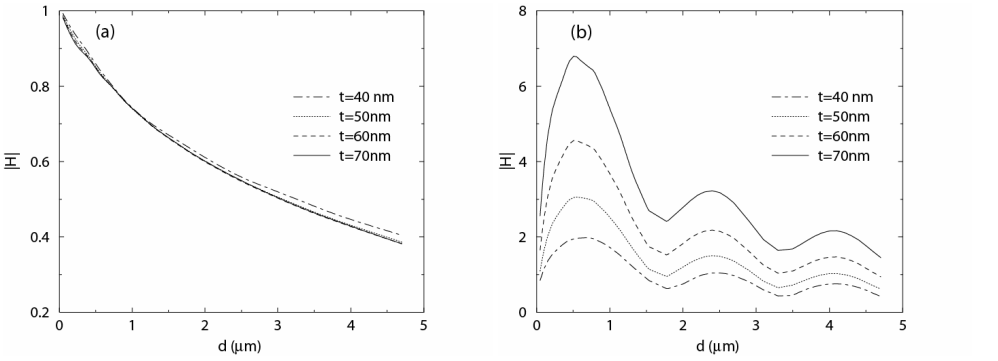

Fig. 4. Relative average amplitude of the field transmitted through the gap measured (a) 5 nm above and (b) 5 nm below the metallic film, as a function of the interruption length d in the film. The air mode is used for excitation, see Fig. 1(a).

#81890 - $15.00 USD Received 6 Apr 2007; revised 7 May 2007; accepted 7 May 2007; published 8 May 2007

To verify this hypothesis, a series of simulations were performed using a higher index substrate with n_{dense_glass}=1.8. The results are shown in Fig. 5, where the relative transmitted amplitude is reported for both substrates. The higher index substrate leads indeed to a smaller oscillation period for the transmittivity: $b_2=\lambda_{air}/(n_{dense\_glass}-1)$=981 nm, as observed in Fig. 5. This confirms the hypothesis that the crosstalks between the two SPP modes through the gap results from the scattering of the incident plasmon both through the air and the glass. When these two scattered waves are in phase, the excitation of the new mode is maximum.

The thickness of the metallic film has a different influence on the tunneling and cross-coupling of the modes. Figure 4(a) indicates that it barely influences the tunneling: for long gaps the transmission is only slightly better for a thin film [t=40 nm, Fig. 4(a)] than it is for a thick film [t=70 nm, Fig. 4(a)]. The origin of this phenomenon is probably the weaker scattering that occurs at the film termination when the film is thin. Hence the energy flow remains more focused in that case. On the other hand, Fig. 4(b) indicates that the cross-coupling from the air mode to the substrate mode is much more effective for a thick metallic film. Again scattering at the edges of the gap is likely to be responsible for this: a thick edge increasing the scattering and leading to stronger cross-coupling.

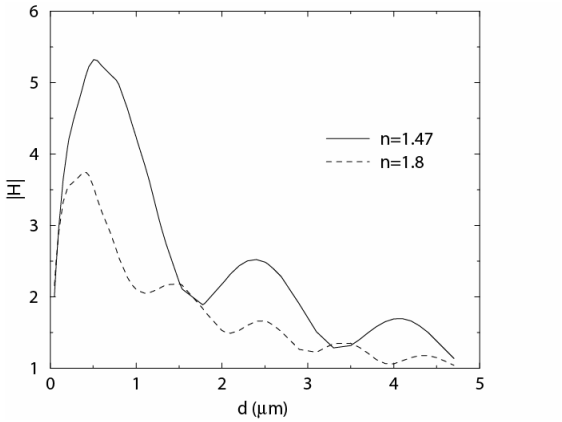

Fig. 5. Relative average amplitude of the field transmitted through the gap measured 5 nm below the metallic film, as a function of the interruption length d in the film. Two different substrates are considered, with respective index n=1.47 and n=1.8.

Let us now consider the case when the structure is illuminated with a substrate mode, see Fig. 1(b). In this case the relative average transmitted magnetic field amplitude gives converse results, as shown in Fig. 6. The field amplitude above the metallic film now periodically varies, Fig. 6(a), while that below the film gradually decreases with the gap length, Fig. 6(b). In contrast to Fig. 4(a), which shows a smooth exponential decay, a subtle modulation is now visible in Fig. 6(b). This modulation is caused by the air mode that radiates into the glass substrate and is also detected when computing the amplitude of the field under the film. Hence, the modulation in Fig. 6(b) corresponds to the residuals of the air mode observed in Fig. 6(a), which spreads into the substrate. One can also notice that the signal in Fig. 6(b) is defined by the sum of the air and glass modes up to d=2 μm. For larger gaps, only the air mode is contributing, since the glass mode decays 2.5 times faster.

#81890 - $15.00 USD Received 6 Apr 2007; revised 7 May 2007; accepted 7 May 2007; published 8 May 2007

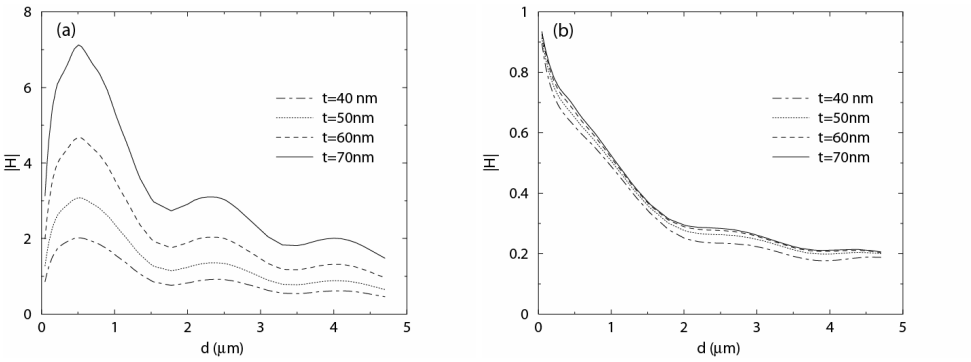

Fig. 6. Relative average amplitude of the field transmitted through the gap measured (a) 5 nm above and (b) 5 nm below the metallic film, as a function of the interruption length *d* in the film. The glass mode is used for excitation, see Fig. 1(b).

2.2. Symmetrical geometry

For applications in information technology, another important geometry class is that where the metallic waveguide is embedded between two similar dielectric layers, leading to a symmetrical geometry (Fig. 7). Two SPP modes can also propagate in such a structure: a so-called long-range (LR) mode, Fig. 7(a), which has a small decay constant and therefore propagates for long distances, thus being used for telecom applications and a short-range (SR) mode, Fig. 7(b), which typically decays fast and it is not of great practical use [1,2,9,11].

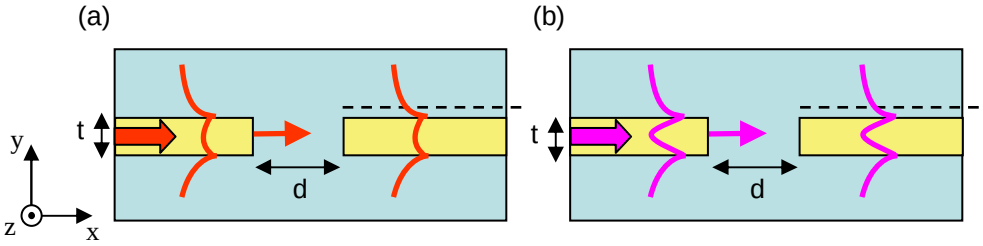

Fig. 7. Symmetrical geometry where a metallic waveguide with thickness *t* and an interruption *d* is embedded in two similar dielectrics. Two SPP modes can propagate in that system: (a) long-range mode and (b) short-range mode. The amplitude of the magnetic field is sketched and any reflected mode is omitted for clarity.

Since the propagation distance of the LR mode increases when the metal thickness decreases, let us consider a thin gold film with thickness t=40 nm embedded between two layers of glass (n_{glass}=1.47). For comparison with the non-symmetrical case, the same illumination wavelength is used: λ=785 nm. The two SPP have following propagation constants (in unit of the vacuum wave number): k_{LR}=1.51-0.0011*i and k_{SR}=1.62-0.0171*i.

Figure 8 gives the amplitude distribution of the magnetic field when a LR mode propagates on a gold film with an interruption d=700 nm. The movie linked to Fig. 8 shows the scattering of the magnetic field when the interruption length changes from d=50 nm to d=4.7 µm. Comparing Figs. 2 and 8 illustrates how well the LR mode can tunnel in this symmetrical configuration: the energy remains "focused" along the direction of the guide, with minimal lateral scattering. Remark in the movie the strong standing wave pattern in the gap – even for very long interruptions – also indicative that the field remains concentrated along the film axis in that system.

#81890 - $15.00 USD Received 6 Apr 2007; revised 7 May 2007; accepted 7 May 2007; published 8 May 2007

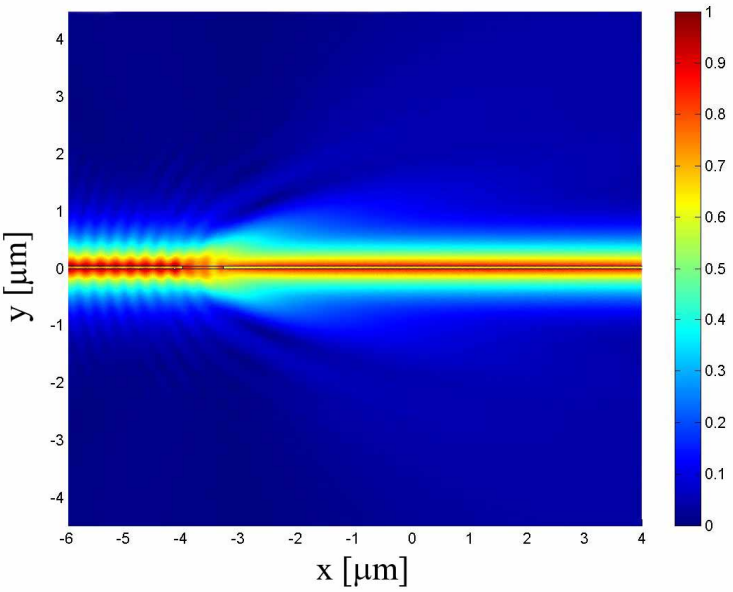

Fig. 8. Amplitude of magnetic field when a LR SPP mode is propagating on a t=40 nm thick gold film with a d=700 nm interruption, see Fig. 7(a). The movie shows the field distribution for interruptions between d=50 nm and d=4.7 μm.

To investigate the transmission and scattering of the SPP in this symmetrical geometry, we show in Fig. 9 the amplitude of the magnetic field 5 nm above the metallic film for LR and SR mode excitations. Since each mode now extends on both sides of the metallic film, it is not possible anymore to distinguish one mode by measuring on a specific side of the film.

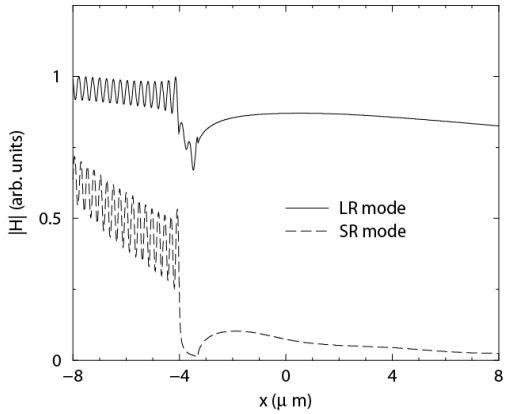

Fig. 9. Amplitude of the magnetic field 5 nm above the t=40 nm thick metallic film (see the dashed lines in Fig. 7) for long-range (LR) and short-range (SR) excitations. The film has a d=700 nm long interruption.

The standing wave caused by the reflection of the incident wave is observed in front of the interruption (compare Figs. 9 and 3). The much faster decay of the SR mode compared to the LR one is also clearly visible in front of the interruption in Fig. 9. Furthermore, the transmission through the gap appears to be much more efficient for the LR mode than for the SR one. Actually, the decay rate of the field transmitted through the gap for SR illumination is

#81890 - $15.00 USD Received 6 Apr 2007; revised 7 May 2007; accepted 7 May 2007; published 8 May 2007

typical of a LR mode (Fig. 9). Thus, in that case, the SR mode excites the LR one through the gap and most of the energy remains in that LR mode after the interruption. Contrary to Fig. 3, no interference pattern is visible in the transmitted field in Fig. 9, confirming that mainly one mode (the LR one) propagates after the gap.

To quantify the transmission of the SR and LR modes over the interruption, the relative amplitude of the transmitted field is shown as a function of the interruption distance *d* in Fig. 10. Note that the LR mode can tunnel through very long gaps with minimal loses. This effect is even stronger for longer wavelengths and thinner metallic films, since in this case the LR mode becomes even less bound to the metal and approaches a free propagating wave (not shown).

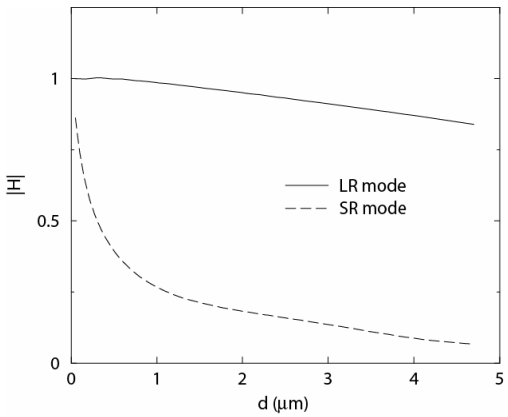

Fig. 10. Relative average amplitude of the field transmitted through the gap measured 5 nm above the metallic film, as a function of the interruption length *d* in the film. Both excitations with LR and SR modes are investigated.

3. Conclusion

We have studied in details the tunneling of surface plasmon-polaritons (SPPs) across an interruption in the metallic film supporting them. Both non-symmetrical and symmetrical geometries have been investigated. In the former, a high tunneling efficiency is observed, with amplitude transmission in excess of 0.5 for gaps as long as 2 μm. This transmission is even higher in the symmetrical case, where the amplitude of the long-range plasmon decays only by about 20% over a 5 μm gap. On the other hand, the transmission is very weak in that system for the short-range plasmon.

In addition to the transmission of the original mode through the gap, we have studied the excitation of additional SPP modes via scattering through the gap. This mode cross-coupling depends periodically upon the gap length and can be explained by the interference between the waves propagating in the substrate and cap layers. This cross-coupling phenomenon can find useful applications for the integration of SPP components for optical signal processing.

Overall, our results indicate that SPPs are not very sensitive to technological imperfections and can survive relatively large waveguide interruptions. This is good news for the practical integration of metallic waveguides in a variety of photonic systems.

Acknowledgments

Funding from the Swiss National Center of Competence in Research Quantum Photonics and the European Network of Excellence Plasmo-nano-devices (FP6-2002-IST-1-507879IST) is gratefully acknowledged.

#81890 - $15.00 USD Received 6 Apr 2007; revised 7 May 2007; accepted 7 May 2007; published 8 May 2007